JOURNAL OF PHYSICAL ORGANIC CHEMISTRY
J. Phys. Org. Chem. 2007; **20:** 1043–1049
Published online 23 August 2007 in Wiley InterScience
(www.interscience.wiley.com) DOI: 10.1002/poc.1250

Mechanism of 4-methyl-1,2,4-triazol-3-thiole reaction with formaldehyde. A DFT study

Monika Wujec[1] and Piotr Paneth[2]*

[1]Department of Organic Chemistry, Faculty of Pharmacy, Medical University, Staszica 6, 20-081 Lublin, Poland
[2]Institute of Applied Radiation Chemistry, Technical University of Lodz, Zeromskiego 116, 90-924 Lodz, Poland

Received 23 March 2007; revised 11 July 2007; accepted 12 July 2007

ABSTRACT: Contrary to the typical nucleophilic substitution, occurring on the sulfur atom of 4-methyl-1,2,4-triazol-3-thiole, the reaction with formaldehyde leads to the formation of the N—C bond rather than the S—C bond. The mechanism of this reaction has been characterized theoretically. Calculations indicate that the reaction proceeds via a cyclic transition state involving one solvent molecule with the Gibbs free activation energy of only 2 kcal/mol. The alternative pathway that leads to the S—C bond formation is about 5 kcal/mol more energetically demanding. Copyright © 2007 John Wiley & Sons, Ltd.
Supplementary electronic material for this paper is available in Wiley InterScience at http://www.mrw.interscience.wiley.com/suppmat/0894-3230/suppmat/

KEYWORDS: 1,2,4-triazole; tautomerization; DFT; theoretical calculations

INTRODUCTION

1,2,4-Triazole and its derivatives constitute an important class of organic compounds with diverse biological activities, such as anticonvulsant, antidepressant, anti-inflammatory, antitumor, analgesic, antiviral, and antibacterial.[1] Therefore, some of them are approved as drugs, for example, alprazolam,[2] etizolam,[3] or vibrunazole.[4] Recently, much attention has been focused on derivatives of 1,2,4-triazole because of their fungicidal activities. They are also used as intermediates for the synthesis of antifungal agents such as fluconazole, voriconazole, and itraconazole.[5] Because of the continuing interest in the biological activity of these compounds, we have synthesized new analogs with promising pharmacological activity.[6,7] Following a literature report[8] indicating that the substitution proceeds via the nucleophilic attack of the sulfur atom, as illustrated in Scheme 1, we have reacted 4-methyl-1,2,4-triazol-3-thiole (**S_{SH}**) with formalin at 25 °C. Formalin is an aqueous solution in which the predominant form is the mono-hydrate, $CH_2(OH)_2$,[9] that is, however, unreactive, and it is free formaldehyde, present in smaller quantity, that is the reactive species. Thus, we consider that reactions under consideration here proceed with formaldehyde, the abundance of which is maintained in solution via rapid equilibrium with formol.

**Correspondence to:* P. Paneth, Institute of Applied Radiation Chemistry, Technical University of Lodz, Zeromskiego 116, 90-924 Lodz, Poland.
E-mail: paneth@p.lodz.pl

Under our experimental conditions, N^1-hydroxymethyl-4-methyl-1,2,4-triazol-5-thione (**P_{NC}** in Scheme 2) turned out to be the sole product. While similar reaction outcomes has been observed in 2-mercaptoimidazoles reacting with carbonyl groups,[10] to the best of our knowledge its mechanism has not been addressed. Furthermore, despite extensive studies of 1-methyl-2-mercaptoimidazole and 1-methylimidazole-2-thione chemistry their tautomeric equilibrium has not been determined conclusively,[11] and they are frequently referred to collectively as methimazole.

We present theoretical calculations that explain 1,2,4-triazol-3-thiole reactivity and provide details of the corresponding transition state that leads to the *N*-substituted derivative. It is shown that this reaction is dominating because its activation energy is a few kcal/mol lower than that of the water-mediated tautomerization that leads to the nitrogen-protonated form, which is required for the reaction that leads to the *S*-substituted product.

RESULTS AND DISCUSSION

All calculations have been carried out at the density functional theory (DFT) level using B3LYP functional.[12] All geometries were initially optimized in the gas phase, but since experimentally the reaction was carried out in formalin, gas-phase geometries were reoptimized in solution as approximated by the PCM implicit solvent

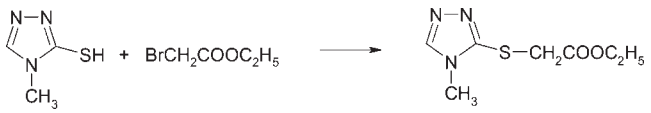

Scheme 1.

model with UFF radii on all atoms (including hydrogen atoms) and with parameters for water.[13] It has been shown that the dielectric properties of the formalin solution are close to that of pure water.[14] Although both geometries and relative energies are not notably perturbed by the introduction of the solvent model, we are discussing results obtained with the PCM solvent model included.

The substrate, 1,2,4-triazol-3-thiole, can exist in either the thiole form, or *N*-protonated tautomeric forms, as shown in Scheme 3. We will refer to the most stable of the *N*-protonated forms as the thione form, $\mathbf{S_{NH}}$.

Thus, the first problem that has to be solved is to determine, which of these forms is present under our reaction conditions. Theoretical calculations for this (results presented herein) and similar systems[11b] indicate that the thione form $\mathbf{S_{NH}}$ is more stable than $\mathbf{S_{SH}}$ by about 10 kcal/mol. These calculations are in agreement with the experimental observation that the thione form is predominantly observed in crystals. Also 1,2,4-triazol-3-thiole crystallizes from water in the thione form.[15] The commercial substrate that has been used, however, is reported to be the $\mathbf{S_{SH}}$ tautomer based on IR and Raman spectra. Since these spectra are not fully conclusive, we have carried out NMR analysis. ^{1}H, ^{13}C, ^{15}N, and 2D ^{1}H–^{15}N correlation NMR spectra provided evidence that the broad signal at 13.4 ppm is not that of the proton attached to any of the nitrogen atoms upon dissolution of this reactant in DMSO or in water/methanol (1:1 vol.). All signals in the ^{15}N spectrum were identified and showed coupling constants of less than 13 Hz (as described in section Experimental Methods), which indicates[16] the absence of the N—H bond. However, after several days the spectra changed; the coupling constant of the ^{15}N signal at 204.9 ppm changed to 107.0 Hz and the signal at 13.4 ppm in the proton spectra became sharp. Proton-decoupled ^{15}N spectrum confirmed the signal at 204.9 ppm to be a doublet and not two singlet signals of similar chemical shift. The ^{13}C spectrum showed a signal at 166.5 ppm, which is characteristic for the C═S bond. These observations together indicated that the tautomerization occurred in the sample and that the only form present is now the $\mathbf{S_{NH}}$ tautomer. This suggests that, under our experimental conditions (as described in Experimental Methods, Reaction conditions), only the thiole form $\mathbf{S_{SH}}$ is present in the solution.

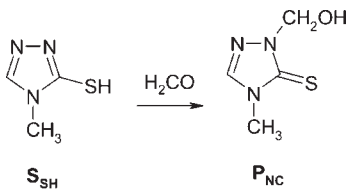

Scheme 2.

Several mechanistic scenarios have been considered. The simplest mechanism involves only the molecules of the two reactants. The DFT-optimized structure of the transition state corresponding to the reaction given in Scheme 2 ($\mathbf{TS_{SH\text{-}NC}}$) is illustrated in Figure 1 and its main geometric and energetic features are collected in Table 1. It is characterized by one imaginary frequency of $229.3i\,\mathrm{cm}^{-1}$ that corresponds predominantly to the motion of the triazole nitrogen atom and formaldehyde carbon atom that leads to the formation of the new bond. The other main contribution to this vibration comes from the proton transfer between sulfur and oxygen atoms. Gibbs free activation energy corresponding to this transition state is equal to only 3.1 kcal/mol. The long bond distance between the nitrogen atom and formaldehyde carbon atom and especially much longer O—H distance compared to S—H distance, in terms of the More O'Ferrall–Albery-Jencks reaction coordinate diagram indicate that it is a very early transition state.[17]

A reaction route competitive to that shown in Scheme 2 consists of tautomerization to the *N*-protonated form followed by the reaction leading to the formation of the S—C bond, as presented in Scheme 4. We have studied theoretically both steps of this route. The first step can proceed either intermolecularly or with the involvement of water molecule(s). The Gibbs free energy of activation for the intramolecular tautomerization (via $\mathbf{TS_{SH\text{-}NH}}$ not shown) exceeds 33 kcal/mol and therefore this mechanism has not been included in the considerations (although this intramolecular mechanism of proton transfer can operate in nonaqueous, aprotic solution of the reactant $\mathbf{S_{SH}}$ as implied by the NMR results). The transition state for the tautomerization pathway that involves one water molecule ($\mathbf{TS_{SHaqNH}}$) is shown in Figure 1. Its imaginary frequency of about $1021i\,\mathrm{cm}^{-1}$ corresponds to simultaneous transfer of two protons: from the thiole group to

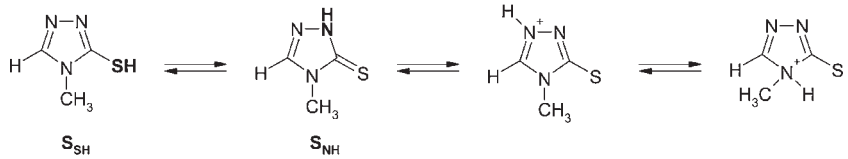

Scheme 3.

DOI: 10.1002/poc

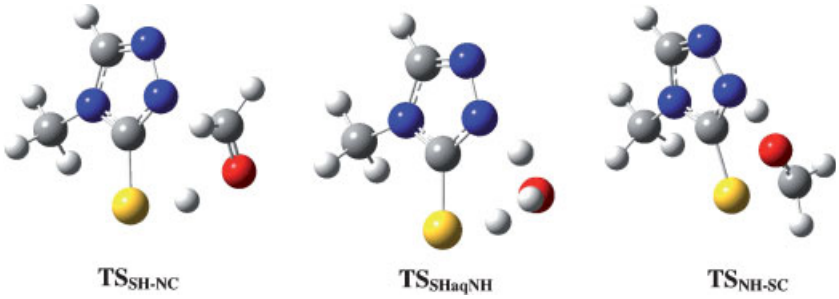

Figure 1. Transition state structures for the reaction given in Scheme 2 (**TS$_{SH-NC}$**) and first (**TS$_{SHaqNH}$**) and second (**TS$_{NH-SC}$**) steps of Scheme 4

the water molecule, and from the water oxygen atom to the nitrogen atom of triazole. The water molecule forms with the N and S centers of the triazole a six-membered ring via the protons in flight. Bond distances to these protons indicate that the process is practically synchronous.

Subsequent reaction of the *N*-protonated tautomer **S$_{NH}$** to the product with the S—C bond formed (**P$_{SC}$**) proceeds through a cyclic transition state analogous to that found for the reaction given in Scheme 2. Its structure is illustrated in Figure 1, while details of the main geometrical parameters and Gibbs free energy of activation are given in the last column of Table 1. Unlike **TS$_{SH-NC}$**, the transition state **TS$_{NH-SC}$** is characterized by an imaginary frequency of the magnitude similar to that of **TS$_{SHaqNH}$**. Its analysis indicates that proton transfer between nitrogen and oxygen atoms is the main contributor to this vibration. The other significant component comes from the movement of sulfur and formaldehyde carbon atoms that close the ring by forming the new S—C bond. The long S—C distance together with the longer O—H than N—H bond indicates that this transition state is closer to reactants than to the product (an early transition state).

Table 1. Bond distances (Å), valence and dihedral angles (°) of atoms involved in six-member cycles of transition state structures, Gibbs free activation energies, and imaginary frequencies

Coordinate/property				**TS$_{SH-NC}$**	**TS$_{SHaqNH}$**	**TS$_{NH-SC}$**
N	H			—	1.613	1.200
S	H			1.380	1.660	—
O[a]	H			1.818	1.039(N)/1.221(S)	1.302
N	C			1.919	—	—
S	C			—	—	2.109
N	H	O		—	146.7	151.2
S	H	O		150.7	157.9	—
S	C	N	C	4.95	—	—
S	C	N	H	—	−1.1	−6.1
N	C	S	C	—	—	−11.8
N	C	S	H	−11.4	0.9	—
C	N	H	O	—	5.1	−2.5
C	S	H	O	−10.5	−5.4	—
$\Delta G^{\neq}$ (kcal/mol)				3.1	6.4	8.2
$i\nu^{\neq}$ (cm^{-1})				229.3	1021.1	1082.1

[a] Oxygen atom of water in case of **TS$_{SHaqNH}$** and of formaldehyde in case of **TS$_{SH-NC}$** and **TS$_{NH-SC}$**.

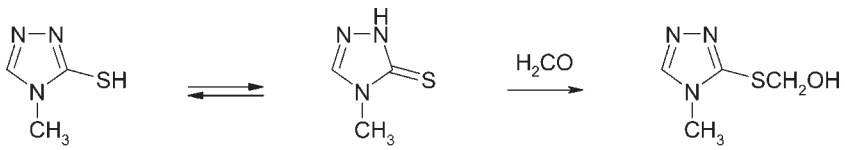

S$_{SH}$ **S$_{NH}$** **P$_{SC}$**

Scheme 4.

DOI: 10.1002/poc

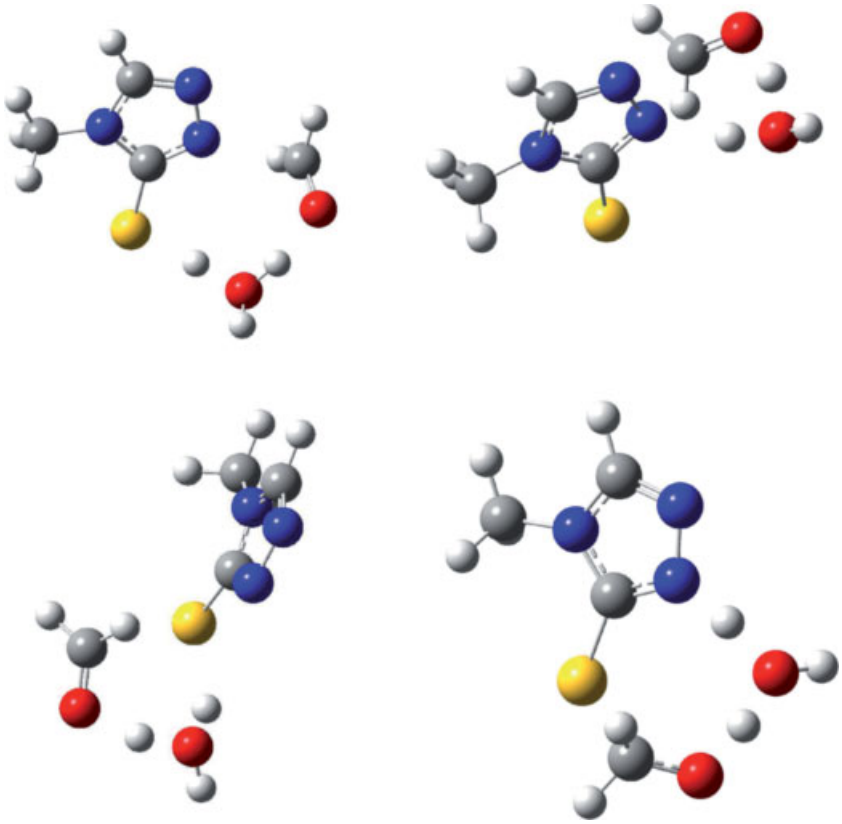

Figure 2. Transition state structures involving a solvent molecule for the reactions given in Scheme 2 (top left: $\mathbf{TS_{SHaqNC}}$) and the second step of Scheme 4 (bottom right: $\mathbf{TS_{NHaqSC}}$), as well as $\mathbf{TS_{NHaqNC}}$ (top right) and $\mathbf{TS_{SHaqSC}}$ (bottom left)

A similar mechanism that leads from the thiole reactant to N—C containing product involves participation of a solvent molecule. The optimized structure of the corresponding transition state ($\mathbf{TS_{SHaqNC}}$) is illustrated in Figure 2. The geometrical features of this transition state are collected in Table 2. The Gibbs free activation energy for this mechanism is only 1.9 kcal/mol, and, therefore, this reaction is more favorable than the reaction between $\mathbf{S_{SH}}$ and formaldehyde alone. Inclusion of one water molecule in the transition state for the reaction leading from the $\mathbf{S_{NH}}$ tautomer to $\mathbf{P_{SC}}$ product ($\mathbf{TS_{NHaqSC}}$) does not alter significantly the barrier, which is equal to 8.4 kcal/mol. In agreement with the Hammond postulate, $\mathbf{TS_{SHaqNC}}$ is an early transition state: the Wiberg bond

Table 2. Bond distances (Å), valence and dihedral angles (°) of atoms involved in eight-member cycles of transition state structures, Gibbs free activation energies, and imaginary frequencies

Coordinate/property			$\mathbf{TS_{SHaqNC}}$	$\mathbf{TS_{NHaqNC}}$	$\mathbf{TS_{SHaqSC}}$	$\mathbf{TS_{NHaqSC}}$
N	H		—	1.721	—	1.212
S	H		1.384	—	2.034	—
C[a]	S		1.757	1.709	1.747	1.741
O[b]	H		1.007	1.019	1.032	1.280
O[c]	H		1.628	1.314	1.352	1.253
N	C		1.922	2.164	—	—
S	C[d]		—	—	2.817	2.082
N	H	O[c]	—	151.4	—	173.1
S	H	O[c]	176.1	—	155.9	—
O[b]	H	O[c]	167.7	156.0	160.0	171.1
$\Delta G^{\neq}$ (kcal/mol)			1.9	25.0	11.7	8.4
$i\nu^{\neq}$ (cm^{-1})			194.6	561.3	240.5	1164.9

[a] Carbon atom of the ring.
[b] Oxygen atom of formaldehyde.
[c] Oxygen atom of water.
[d] Carbon atom of formaldehyde.

DOI: 10.1002/poc

order[18] of the breaking S—H bond is 0.85 while the bond order of the forming N—C bond that closes the ring is only 0.42, and bond orders in the relay that transfers proton from the reactant to the oxygen atom of formaldehyde are 0.09, 0.60, and 0.12, respectively. Bond orders of the breaking N—H bond and forming S—C bond in $\mathbf{TS_{NHaqSC}}$, on the other hand, are 0.43 and 0.74, respectively, indicating a late transition state. The proton relay system in this transition structure is more balanced, with bond orders equal to 0.30, 0.39, and 0.32 in the direction toward the oxygen atom of formaldehyde.

In models considered thus far, the new bond to the formaldehyde carbon is formed by the atom (nitrogen or sulfur) which lacks the proton. However, it may be envisioned that a protonated atom forms the new bond with the carbon atom of formaldehyde. Again, such a mechanism requires intervention of a solvent molecule. We have identified two such transition states. The first one, $\mathbf{TS_{NHaqNC}}$, corresponds to the reaction leading from the $\mathbf{S_{NH}}$ tautomer to the product containing a N—C bond ($\mathbf{P_{NC}}$). Analogously, the second one ($\mathbf{TS_{SHaqSC}}$) corresponds to the reaction from $\mathbf{S_{SH}}$ to $\mathbf{P_{SC}}$. Both these structures are characterized in Figure 2 and Table 2.

Finally, since thiolates are powerful nucleophiles, thus one might expect that the thiolate of the reactant ($\mathbf{S_{S^-}}$) may compete with the protonated species for formaldehyde. Although the 1,2,4-triazol-3-thiole system does not deprotonate in water (the anion can only be obtained upon treatment with a very strong base), we have evaluated the energetics of such reaction (data not shown). Gibbs free energy of activation for the reaction between the thiolate and formaldehyde is 2.7 kcal/mol, which again is higher than the reaction involving one water molecule and neutral reactants.

The energetics of the reactions considered in the present study that are relevant to reactivity observed experimentally are presented in Figure 3. Reactants and products shown in this figure for both addition reactions were obtained by optimization of the end-points of the IRC calculations[19] starting from $\mathbf{TS_{SHaqNC}}$ and $\mathbf{TS_{NHaqSC}}$ transition structures. Thus in both cases the models included triazole, formaldehyde, and water molecules. In the studies of tautomerization, on the other hand, formaldehyde molecule was not included. The sum of Gibbs free energies of formaldehyde and the binary triazole–water complexes of tautomeric $\mathbf{S_{SHaq}}$ and $\mathbf{S_{NHaq}}$ forms are within about 1.5 kcal/mol of the Gibbs free energies of the corresponding ternary complexes $\mathbf{S_{SHaq}\cdot H_2CO}$ and $\mathbf{S_{NHaq}\cdot H_2CO}$. For clarity, these differences are omitted in Figure 3 and indicated only by the discontinuity of the corresponding energy levels.

The Gibbs free energy of activation for the first step of the pathway given by Scheme 3, tautomerization of the substrate, is 6.5 kcal/mol, that is, 4.6 kcal/mol larger than for the competitive reaction that leads to the N—C bond formation (Scheme 2). The Gibbs free energy of activation for the subsequent step, leading to $\mathbf{P_{SC}}$ is 8.4 kcal/mol. Thus for the reaction that originates in the thiole

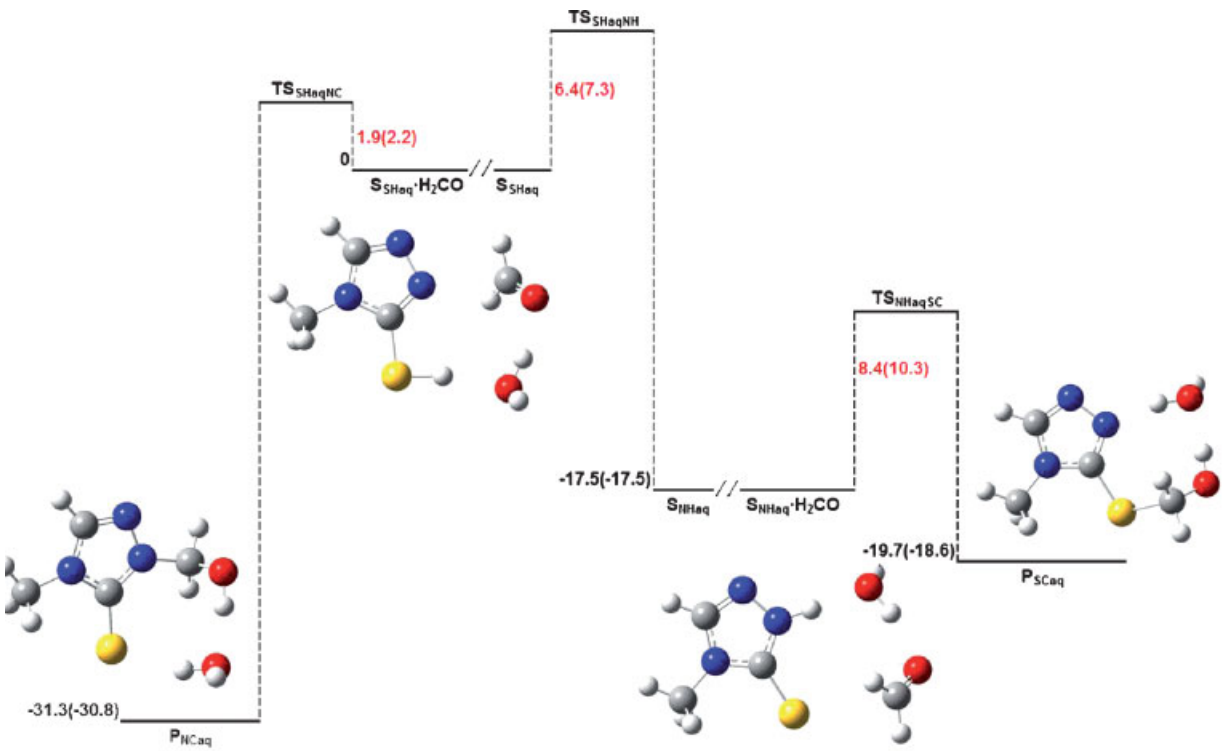

Figure 3. Gibbs free energy profile of reactions considered. Relative energies (kcal/mol) are shown in black, and activation energies are shown in red

DOI: 10.1002/poc

tautomer of the reactant, the kinetically preferred direction is toward the $\mathbf{P_{NC}}$ product with the N—C bond formed, as observed experimentally. Explicit inclusion of one water molecule lowers the Gibbs free energy of activation of the reaction of $\mathbf{S_{SH}}$ in the experimentally observed direction toward $\mathbf{P_{NC}}$ by 1.2 kcal/mol. The same direction of the reaction is favored in the thermodynamic control since the Gibbs free energy difference between $\mathbf{S_{SH}}$ and $\mathbf{P_{SC}}$ is 19.7 kcal/mol while between $\mathbf{S_{SH}}$ and $\mathbf{P_{NC}}$ is 31.3 kcal/mol. Energy calculations with larger basis set are reported in Figure 3 in parenthesis. They do not alter the energetic landscape presented above.

In summary, we have shown computationally that in agreement with experimental observations the reaction between 4-methyl-1,2,4-triazol-3-thiole and formaldehyde leads to N^1-hydroxymethyl-4-methyl-1,2,4-triazol-5-thione. This pathway is favored both kinetically, Gibbs free energy of activation of only 1.9 kcal/mol, and thermodynamically, Gibbs free energy difference of 31.3 kcal/mol. The cyclic transition state for this reaction includes both reactants and one explicit water molecule that is involved in the proton relay system.

EXPERIMENTAL METHODS

Materials

4-Methyl-1,2,4-triazol-3-thiole and formaldehyde (37%) were obtained from commercial supplier. The purity was checked by TLC on Aluminum oxide 60 F_{254} plates (Merck) in a $CHCl_3/C_2H_5OH$ (10:1 and 4:1) with UV visualization. Melting points were determined in Fisher–Johns blocks. The results of elemental analyses for C, H, and N were within ±0.4% of the theoretical values. ^{1}H, ^{13}C, and ^{15}N NMR spectra were recorded in DMSO-d_6 and in the water/methanol mixture (1:1) at 303 K on a spectrometer operated at 700.08 MHz for ^{1}H NMR, corresponding to 176.5 and 70.95 MHz for ^{13}C and ^{15}N nuclei, respectively. The nitrogen chemical shifts were assigned on the basis of HMQC experiments. ^{1}H NMR (DMSO) δ 3.37 (s, 3H, CH_3); 8.23 (d, 2H, $J = 7.5$ Hz, CH); 13.41 (s, 1H, SH). ^{13}C NMR (DMSO) δ 31.5 (CH_3), 142.6 (CH), 166.5 (C). ^{15}N NMR (DMSO) δ 168.6 (dq, $J = 6.9$, 2.0 Hz, N—CH_3), 204.9 (d, $J = 5.3$ Hz, N═C—SH), 278.3 (d, $J = 13.3$ Hz, N═CH).

Reaction conditions

4-Methyl-1,2,4-triazol-3-thiole (0.01 mole) and 0.01 mole of formaldehyde solution (37%) were mixed and left at room temperature (25 °C) for ½ h. The obtained product was filtered, dried, and crystallized from ethanol. Yield 85%. M.p. 125–126 °C. $C_4H_7N_3OS = 145.184$. ^{1}H NMR (DMSO) δ 3.47 (s, 3H, CH_3); 5.36 (d, 2H, $J = 7.5$ Hz, CH_2); 6.79 (t, 1H, $J = 7.5$ Hz, OH); 8.48 (s, 1H, CH). ^{13}C NMR (DMSO) δ 32.1 (CH_3), 70.5 (CH_2), 141.5 (CH), 166.2 (C). ^{15}N NMR (DMSO) δ 169.9 (d, $J = 8.1$ Hz, N—CH_3), 206.3 (d, $J = 5.6$ Hz, N═C—SH), 279.5 (d, $J = 13.1$ Hz, N═CH).

Computational methods

DFT calculations were performed. Geometry optimization of reactants, transition states, and products was carried out using the B3LYP functional[12] and the standard 6-31+G(d,p) basis set[20] as implemented in the Gaussian 03 package.[21] All calculations were carried out using default convergence criteria. Vibrational analysis was performed for the optimized structures to confirm that they represent stationary points on the potential energy surfaces (3n-6 real normal modes of vibration for the reactant and one imaginary frequency for the transition state). Gas phase geometries were subsequently reoptimized using the same theory level and basis set, and the PCM implicit solvent model with parameters corresponding to water.[13] Gibbs free energy values correspond to a temperature of 298 K. ZPE contributions to energy barriers were about −1.9 kcal/mol. UFF[22] radii of all atoms, including hydrogen atoms, were used in the cavity building. For complexes including water molecules, once the transition structures were optimized the IRC protocol[19] was used to identify reactants and products of the corresponding reaction. Structures obtained from these calculations were subsequently optimized to the nearest stationary points and vibrational analysis was used to confirm that they represent minima on the potential energy surface. Energy calculations at the B3LYP/6-311++G(d,p) level[23] do not introduce significant changes to the profiles of the studied reactions. The values from this theory level are given in Figure 3.

SUPPORT INFORMATION

Optimized geometries of the reactants, products, and transition state structures are available online in Wiley InterScience at http://www.mrw.interscience.wiley.com/suppmat/0894-3230/suppmat/.

Acknowledgements

Access to supercomputing facilities at Cyfronet, Karkow, and PSSC Poznan, Poland is greatfully acknowledged. We thank Prof. Stefan Jankowski and Prof. Zbigniew Kaminski for helpful discussions and Adam Mazur for help with NMR analysis.

REFERENCES

1. (a) Husain MI, Amir M. *J. Indian Chem. Soc.* 1986; **63**: 317–319; (b) Chiu S-HL, Huskey S-EW. *Drug Metab. Dispos.* 1998; **26**: 838–847; (c) Sahin G, Palaska E, Kelicen P, Demirdamar R, Altmok G. *Arzneim. -Forsch./Drug Res.* 2001; **51**: 478–484; (d) Al-Soud YA, Al-Dweri MN, Al-Masoudi NA. *Il Farmaco* 2004;

DOI: 10.1002/poc

59: 775–783; (e) Mekuskiene G, Gaidelis P, Vainilavicius P. *Pharmazie* 1998; **53**: 94–96; (f) Papakonstantinou-Garoufalias SS, Tani E, Todoulou O, Papadaki-Valiraki A, Filippatos E, De Clercq E, Kourounakis PN. *J. Pharm. Pharmacol.* 1998; **50**: 117–124; (g) Pandeya SN, Sriram D, Nath G, De Clercq E. *Arzneim. -Forsch./Drug Res.* 2000; **50**: 55–59.
2. Pick ChG. *Brain Res. Bull.* 1997; **42**: 239–243.
3. Shiroki M, Tahara T, Araki K. Pat. Jap. 75100096, 1975, *Chem. Abstr.* 1976; **84**: 59588k.
4. Holmwood G, Buechel KH, Plempel M, Haller J. Pat. RFN DE 3018865, 1981. *Chem. Abstr.* 1982; **96**: 62979s.
5. (a) Bailey EM, Krakovsky DJ, Rybak M. *J. Pharmacother.* 1990; **10**: 146–153; (b) McGinnis MR, Pasarell L, Sutton DA, Fothergill AW, Cooper CR, Rinaldi MG. *Antimicrob. Agents Chemother.* 1997; **41**: 1832–1834.
6. (a) Wujec M, Pitucha M, Dobosz M, Kosikowska U, Malm A. *Acta Pharm.* 2004; **54**: 251–260; (b) Wujec M, Pitucha M, Dobosz M. *Heterocycles* 2006; **68**: 779–785.
7. Siwek A. Ph.D. Thesis, *Medical Academy*, Lublin, Poland, 2007.
8. Maliszewska-Guz A, Wujec M, Pitucha M, Dobosz M, Chodkowska A, Jagiełło-Wójtowicz E, Mazur L, Kozioł AE. *Collect. Czech. Commun.* 2005; **70**: 51–62.
9. Wade LG. *Organic Chemistry* (5th edn). Person Education, Inc.: Upper Sadle River, NJ, USA, 2003.
10. (a) Heath H, Lawson A, Rimington C. *J. Chem. Soc.* 1951: 2215–2217; (b) Lawson A, Morley HV. *J. Chem. Soc.* 1956: 1103–1108.
11. (a) Guziec LJ, Guziec FS Jr. *J. Org. Chem.* 1994; **59**: 4691–4692; (b) Landry VK, Minoura M, Pang K, Buccella D, Kelly BV, Parkin G. *J. Am. Chem. Soc.* 2006; **128**: 12490–12497.
12. (a) Becke AD. *Phys. Rev. A* 1988; **38**: 3098–3100 and *J. Chem. Phys.* 1993; **98**: 5648–5652; (b) Lee C, Yang W, Parr RG. *Phys. Rev. B* 1988; **37**: 785–789.
13. Miertus S, Scrocco E, Tomasi J. *Chem. Phys.* 1981; **55**: 117–129.
14. Arroyo ST, Martin JAS, Garcia AH. *Chem. Phys.* 2003; **293**: 193–202.
15. El Hajji A, El Ammari L, Mattern G, Benarafa L, Idrissi MS. *J. Chim. Phys. Phys. -Chim. Biol.* 1998; **95**: 2103–2108.
16. Witanowski W, Stefaniak L, Webb GA. In *Nitrogen NMR Spectroscopy*, Webb GA (ed). *Ann. Rep. NMR Spectrom. 18.* Academic Press: London, UK, 1986.
17. (a) More O'Ferrall RA. *J. Chem. Soc. B* 1970; 274; (b) Jencks WP. *Chem. Rev.* 1985; **85**: 511–527.
18. Bochicchio RC, Lain L, Torre A. *Chem. Phys. Lett.* 2003; **374**: 567–571.
19. Gonzalez C, Schlegel HB. *J. Chem. Phys.* 1989; **90**: 2154–2161.
20. (a) Hariharan PC, Pople JA. *Theor. Chim. Acta* 1973; **28**: 213–222; (b) Francl MM, Pietro WJ, Hehre WJ, Binkley JS, Gordon MS, DeFrees DJ, Pople JA. *J. Chem. Phys.* 1982; **77**: 3654–3665.
21. Frisch MJ, Trucks GW, Schlegel HB, Scuseria GE, Robb MA, Cheeseman JR, Montgomery JA Jr, Vreven T, Kudin KN, Burant JC, Millam JM, Iyengar SS, Tomasi J, Barone V, Mennucci B, Cossi M, Scalmani G, Rega N, Petersson GA, Nakatsuji H, Hada M, Ehara M, Toyota K, Fukuda R, Hasegawa J, Ishida M, Nakajima T, Honda Y, Kitao O, Nakai H, Klene M, Li X, Knox JE, Hratchian HP, Cross JB, Bakken V, Adamo C, Jaramillo J, Gomperts R, Stratmann RE, Yazyev O, Austin AJ, Cammi R, Pomelli C, Ochterski JW, Ayala PY, Morokuma K, Voth GA, Salvador P, Dannenberg JJ, Zakrzewski VG, Dapprich S, Daniels AD, Strain MC, Farkas O, Malick DK, Rabuck AD, Raghavachari K, Foresman JB, Ortiz JV, Cui Q, Baboul AG, Clifford S, Cioslowski J, Stefanov BB, Liu G, Liashenko A, Piskorz P, Komaromi I, Martin RL, Fox DJ, Keith T, Al-Laham MA, Peng CY, Nanayakkara A, Challacombe M, Gill PMW, Johnson B, Chen W, Wong MW, Gonzalez C, Pople JA. *Gaussian 03*, Revision D.01, Gaussian Inc., Wallingford, CT, 2004.
22. Rappé AK, Casewit CJ, Colwell KS, Goddard WA III, Skiff WM. *J. Am. Chem. Soc.* 1992; **114**: 10024–10035.
23. Krishnan R, Binkley JS, Seeger R, Pople JA. *J. Chem. Phys.* 1980; **72**: 650–654.

DOI: 10.1002/poc